

Effect of the smectic-*A* temperature range on the behavior of the smectic-*A*—smectic-*C* (or —chiral-smectic-*C*) transition

C. C. Huang and S. C. Lien*

School of Physics and Astronomy, University of Minnesota, Minneapolis, Minnesota 55455

(Received 4 September 1984)

First we demonstrate that the extended mean-field model suggested by Huang and Viner is necessary and sufficient to describe the nature of the smectic-*A*—smectic-*C* (or —chiral-smectic-*C*) transition. The rest of the expansion terms in the mean-field free energy can be treated as higher-order correction terms. Then a general scheme is proposed to normalize the smectic-*C* (or chiral smectic-*C*) order parameter. As a result, the mean-field coefficients near the smectic-*A*—smectic-*C* (or —chiral-smectic-*C*) transition are found to vary systematically with the size of the smectic-*A* temperature range for all single-component liquid-crystal compounds with smectic-*A*—smectic-*C* (or —chiral-smectic-*C*) transition.

I. INTRODUCTION

Liquid crystals are organic molecules, anisotropic in shape, which have one or more mesophases between the crystalline state and the isotropic liquid (*I*). Unlike most materials which have well separated and isolated phase transitions, the phase transitions between different mesophases, in many cases, occur in narrow temperature ranges and can be continuous or weakly first order. Liquid crystals therefore provide a rich variety of orderings and are excellent systems for studying the three-dimensional ($d=3$) aspects of phase transitions as well as the effect of one transition on the other one, in particular, the properties of various multicritical points.

Among the various mesophases, four of them are relevant to our discussion here, nematic (*N*), smectic-*A* (*SmA*), smectic-*C* (*SmC*), and chiral smectic-*C* (*SmC**) phases. In the nematic phase, on average the long axis of each molecule (molecular director) is oriented along a preferred direction. The center of mass of each molecule is, however, free to diffuse throughout the system so that translational invariance is preserved. The *SmA* and the *SmC* phases are characterized by a one-dimensional density wave whose wave vector is along (*A*) or tilted with respect to (*C*), the molecular director. The molecules maintain translational invariance within the smectic planes. If the constituent molecules are optically active, the *SmC** phase will be observed instead of the *SmC* phase. In addition to the direct phase transitions from the isotropic phase to these four mesophases, various phase transitions have been found between the mesophases. Among all these possible phase transitions, at least, *N*-*SmA*, *SmA*-*SmC*, and *SmA*-*SmC** transitions have been demonstrated to be continuous in many liquid-crystal compounds. Thus far, all *N*-*SmA* transitions have large critical regions and the transitions will change from being continuous to being first order as the nematic temperature range decreases.^{1,2} On the other hand, the *SmA*-*SmC* and *SmA*-*SmC** transitions are found to be mean-fieldlike. In two cases,^{3,4} we have reported that one important dimen-

sionless parameter characterizing the *SmA*-*SmC* (or *SmC**) transition is approximately linear function of the size of the *SmA* temperature range. However, among the single-component compounds with the *I*-*N*-*SmA*-*SmC* transition sequence, this dimensionless parameter varies fairly irregularly with the temperature range of the *SmA* phase.⁴ Here we propose a normalization scheme for the *SmC* (or *SmC**) order parameter, calculate the corresponding normalized mean-field coefficients and demonstrate that the size of the *SmA*-temperature range has systematic effect on this new set of normalized mean-field coefficients obtained from all measured single-component liquid-crystal compounds with *SmA*-*SmC* (or *SmC**) transition. Similar analysis has been carried out along the *SmA*-*SmC* transition line of the mixtures of octyloxy-*p*-pentylphenyl and heptyloxy-*p*-pentylphenyl thiolbenzoate (8S5-7S5). When the mixture system approaches the *NAC* point where the *N*, *SmA*, and *SmC* phases coexist, increases in the normalized mean-field coefficients are obtained as before.⁵ This new approach in the extended mean-field theory allows us to gain further insight into the effect on the mean-field coefficients of *SmA*-*SmC* (or *SmC**) transitions as the temperature range of the *SmA* phase decreases. In the next section we will give further justification of the extended mean-field model suggested by Huang and Viner⁶ to describe the *SmA*-*SmC* (or *SmC**) transition by separately including higher-order terms in our heat-capacity fittings. To facilitate the discussion of *SmA*-*SmC* (or *SmC**) transitions of various liquid-crystal compounds, a normalized form of the extended mean-field free energy is proposed in Sec. III. Finally, all the existing high-quality heat-capacity data near the *SmA*-*SmC* (or *SmC**) transition are analyzed and discussed in Sec. IV.

II. THE EXTENDED MEAN-FIELD FREE ENERGY FOR *SmA*-*SmC* (OR *SmC**) TRANSITION

Generally, the free energy near a mean-field transition can be written as

TABLE I. Summary of the heat-capacity data-analyses near the Sm *A*-Sm *C** transition of MBRA8. Here a_1 is set equal to one. *These parameters have been set equal to zero in the given fitting.

Fitting	$10^4 b_0$	$10^6 c_0$	$10^3 a_2$	$10^3 b_1$	$10^9 d_0$	χ^2
I	0.22 ± 0.01	0.54 ± 0.02	*	*	*	0.70
II	0.22 ± 0.01	0.54 ± 0.02	0.14 ± 0.01	*	*	0.69
III	0.22 ± 0.01	0.51 ± 0.02	*	-0.15 ± 0.01	*	0.66
IV	0.22 ± 0.01	0.51 ± 0.02	*	*	0.34 ± 0.02	0.65

$$G = G_0 + a(t)\Psi^2 + b(t)\Psi^4 + c(t)\Psi^6 + d(t)\Psi^8. \quad (1)$$

Here Ψ is the order parameter, $t = (T - T_c)/T_c$ and T_c is the transition temperature. G_0 is the nonsingular part of the free energy. The temperature dependent coefficients can be expressed in Taylor series as follows:

$$a(t) = a_1 t + a_2 t^2 + \dots,$$

$$b(t) = b_0 + b_1 t + \dots,$$

$$c(t) = c_0 + c_1 t + \dots,$$

and

$$d(t) = d_0 + \dots$$

Here, all the coefficients are independent of t and Ψ . Usually, retaining the leading terms (i.e., a_1 and b_0) is sufficient to describe a continuous mean-field transition. All the other terms are higher-order correction terms. Based on one of their high-resolution heat-capacity measurements, Huang and Viner⁶ have proposed an extended mean-field free-energy expression, i.e., including a_1 , b_0 , and c_0 terms to describe the nature of the Sm *A*-Sm *C* transition. Thus far the significance of the c_0 term has been confirmed in all the liquid-crystal compounds being carefully studied near the Sm *A*-Sm *C* (or Sm *C**) transition.^{3,7-14} To test the relative importance of the other terms, i.e., a_2 , b_1 , and d_0 , we have carried out additional three separate fittings to our high-resolution heat-capacity

data by including either the a_2 , b_1 , or d_0 term, respectively, into our data analyses. Here, without losing any generality, the coefficient a_1 was set equal to one through the discussion of this section. Under this circumstance, the order parameter Ψ has the dimensions of (energy/mole)^{1/2}. Table I shows the results of our data analyses near the Sm *A*-Sm *C** transition of S-4-O-(2-methyl-butyl) β -resorcylicidene-4'-*n*-octylaniline (MBRA8). With only 6 K temperature range for the Sm *A* phase, the fluctuations associated with the *I*-Sm *A* transition will have significant effects on the Sm *A*-Sm *C** transition of MBRA8. To find out the relative importance of Ψ^6 and Ψ^8 terms, we analyzed heat-capacity data on MBRA8 first. The fairly consistent values in the coefficient b_0 and c_0 among those four cases and the small decrease in χ^2 values for cases II, III, and IV in comparison with case I indicate that our approach by including a_2 , b_1 , and d_0 separately in the data analyses is a reasonable one. Next, we would like to check the relative importance of each term. The ratios of five expansion terms with respect to the leading term ($|a_1 t \Psi^2|$) are shown in Table II. To demonstrate the effect of the temperature, ratios are calculated at $T_c - T = 0.056$ K (case A) and 14.0 K (case B), respectively. Near T_c (case A), the order parameter Ψ is small, thus $b_0 \Psi^4$ is larger than $c_0 \Psi^6$. On the other hand, away from T_c (case B), Ψ is sufficiently large, $c_0 \Psi^6$ becomes more important than $b_0 \Psi^4$. This suggests that the coefficient c_0 is not small at all. In both limits the c_0 term is at least one order of magnitude larger than a_2 , b_1 ,

TABLE II. The relative magnitudes of five expansion terms in the free energy with respect to $|a_1 t \Psi^2|$ term near the Sm *A*-Sm *C** transition of MBRA8. A is the ratios calculated at $T_c - T = 0.056$ K. B is the ratios calculated at $T_c - T = 14.0$ K.

	$\frac{b_0 \Psi^4}{ a_1 t \Psi^2 }$	$\frac{c_0 \Psi^6}{ a_1 t \Psi^2 }$	$\frac{a_2 t^2 \Psi^2}{ a_1 t \Psi^2 }$	$\frac{b_1 t \Psi^4}{ a_1 t \Psi^2 }$	$\frac{d_0 \Psi^8}{ a_1 t \Psi^2 }$
A	0.44	0.81×10^{-2}	0.24×10^{-7}	-0.54×10^{-3}	0.76×10^{-4}
B	0.74×10^{-1}	0.26	0.61×10^{-5}	-0.23×10^{-1}	0.23×10^{-1}

TABLE III. The relative magnitudes of five expansion terms in the free energy with respect to $|a_1 t \Psi^2|$ in the vicinity of the Sm*A*-Sm*C** transition of 2M45OBC. A is the ratios calculated at $T_c - T = 0.060$ K. B is the ratios calculated at $T_c - T = 9.9$ K.

	$\frac{b_0 \Psi^4}{ a_1 t \Psi^2 }$	$\frac{c_0 \Psi^6}{ a_1 t \Psi^2 }$	$\frac{a_2 t^2 \Psi^2}{ a_1 t \Psi^2 }$	$\frac{b_1 t \Psi^4}{ a_1 t \Psi^2 }$	$\frac{d_0 \Psi^8}{ a_1 t \Psi^2 }$
A	0.42	0.98×10^{-2}	0.15×10^{-5}	0.27×10^{-2}	0.20×10^{-5}
B	0.15	0.22	0.24×10^{-3}	0.17×10^{-2}	0.26×10^{-2}

and d_0 terms. This demonstrates that within fairly wide temperature ranges a_1 , b_0 , and c_0 terms are necessary and sufficient to describe the Sm*A*-Sm*C** transition of MBRA8. The same conclusion can be drawn from similar data analyses on our heat-capacity data near the Sm*A*-Sm*C** and Sm*A*-Sm*C* transitions of chiral and racemic configurations of (2-methyl-butyl)-4'-(*n*-pentyloxybiphenyl)-4-carboxylate (2M45OBC). One of these results is shown in Table III. Again, the result demonstrates that the extended mean-field free energy with a_1 , b_0 , and c_0 terms is necessary and sufficient to describe the Sm*A*-Sm*C** transition of 2M45OBC. In addition, just above the Sm*A*-Sm*C* transition of butyloxybenzylidene heptylaniline (4O.7), the inverse of Sm*C* tilt susceptibility was found to be a linear function of the reduced temperature.¹⁵ On the high-temperature side of the Sm*A*-Sm*C* transition, the Sm*C* tilt susceptibility is inverse proportionally to the coefficient of Ψ^2 in the free-energy expansion (Eq. 1). Thus this is consistent with what we observe here, i.e., the $a_2 t^2$ term is much smaller than the $a_1 t$ term.

III. NORMALIZED EXPRESSION FOR THE EXTENDED MEAN-FIELD FREE ENERGY

In the former section, we have concluded that the following Landau free-energy expression is a very good approximation to describe the Sm*A*-Sm*C* (or Sm*C**) transition

$$G = G_0 + a_1 t \Psi^2 + b_0 \Psi^4 + c_0 \Psi^6. \quad (2)$$

Here the order parameter Ψ describes the molecular tilt angle with respect to the smectic layer normal below the Sm*A*-Sm*C* (or Sm*C**) transition. $t = (T - T_{AC})/T_{AC}$ is the Sm*A*-Sm*C* (or Sm*C**) transition temperature. G_0 is the nonsingular part of the free energy and the constants $(a_1, b_0, c_0) > 0$ (Ref. 16) for a continuous transition. After minimizing G with respect to Ψ , Ψ is zero for $T > T_{AC}$. In the case of $T < T_{AC}$, we have

$$\Psi^2 = R [(1 - 3t/t_0)^{1/2} - 1], \quad (3)$$

where $R = b_0/(3c_0)$ and $t_0 = b_0^2/(a_1 c_0)$. Then the second derivative of G with respect to T leads to the following expression for heat capacity:

$$C = \begin{cases} C_0, & T > T_{AC} \\ C_0 + AT(T_m - T)^{-1/2}, & T < T_{AC}. \end{cases} \quad (4)$$

Here C_0 is the background heat capacity obtained from $G_0, A = a_1^{3/2}/[2(3c_0)^{1/2}T_{AC}^{3/2}]$ and $T_m = T_{AC}(1 + t_0/3)$, where T_{AC} is chosen to be the midpoint of the mean-field heat-capacity jump. In reduced temperature, t_0 is the full width at half height of $(C - C_0)/T$ versus T curve. From Eq. (3), for $|t| \ll t_0, \Psi \sim |t|^{1/2}$ which is the ordinary mean-field-like behavior and for $|t| \gg t_0, \Psi \sim |t|^{1/4}$ which characterizes the mean-field-tricritical-like behavior. Thus the dimensionless parameter t_0 describes the crossover from an ordinary mean-field region near the transition temperature to a mean-field-tricritical-like one away from the transition temperature. In the Sm*A*-Sm*C* (or Sm*C**) transition, the smallness of t_0 value ($\leq 5 \times 10^{-3}$) indicates that mean-field-tricritical-like behavior is important. Thus for $-t < t_0$, in terms of the reduced temperature t , the list of mean-field free-energy expansion terms in increasing order is the following: $b_0 \Psi^4 \sim 0(|t|)$, $a_1 t \Psi^2 \sim c_0 \Psi^6 \sim 0(|t|^{3/2})$, $b_1 t \Psi^4 \sim d_0 \Psi^8 \sim 0(|t|^2)$, and $a_2 t^2 \Psi^2 \sim 0(|t|^{5/2})$. This argument is consistent with the results reported in Sec. II, i.e., b_1 and d_0 terms are smaller and the a_2 term is much smaller than the c_0 term.

Employing heat-capacity and tilt-angle data, we can determine the three leading expansion coefficients in the Landau free energy: $a_1 = 2T_{AC}t_0(\Delta C_J)/(3R)$, $b_0 = a_1 t_0/(3R)$, and $c_0 = b_0/(3R)$. Here, ΔC_J is the mean-field heat-capacity jump at T_{AC} . However, the values of these coefficients still depend on the units used for the order parameter, i.e., tilt angle. Using radian as the natural unit for the tilt angle, we have obtained relatively irregular behaviors between these three coefficients and the range of the Sm*A* phase for the compounds showing *I*-Sm*A*-Sm*C* (or Sm*C**) transition sequence⁴ and the (8S5-7S5) mixtures⁵ while the dimensionless parameter t_0 is approximately linear functions of the Sm*A* temperature range. Consequently, so far t_0 was chosen to illustrate behaviors of Sm*A*-Sm*C* (or Sm*C**) transition as the Sm*A* temperature range varies.^{3,4} However, as t_0 approaches zero, it indicates a large mean-field tricritical-like region but does not necessarily guarantee the existence of a mean-field tricritical point ($b_0 = 0$). Because $t_0 = b_0^2/(a_1 c_0)$, an increase in the values of a_1 and/or c_0 as a function of relevant physical parameters (e.g., Sm*A* temperature range) may force t_0 to decrease toward zero, even though the b_0 value remains constant or even increases slightly. To overcome this difficulty and unambiguously address the possibility of mean-field tricritical points, here we propose a unique way to determine the mean-field free-energy coefficients. The saturated tilt angle for $T \ll T_{AC}$

TABLE IV. The parameters obtained from heat-capacity measurements near the Sm *A*-Sm *C* (or Sm *C*^{*}) transitions of the compounds with the *I*-Sm *A*-Sm *C* (or Sm *C*^{*}) transition sequence.

Compound	T_{AC} (K)	T_{IA} (K)	$1 - \frac{T_{AC}}{T_{IA}}$	$t_0 \times 10^3$	ΔC_J^a	\tilde{a}^b	\tilde{b}^b	References
HOBACPC	353.240	409.2	0.137	5	2.8×10^2	8100	330	11
2M45OBC(<i>R</i>)	316.004	336.96	0.062	3.9	1.24×10^2	2830	102	12
2M45OBC(<i>C</i>)	316.350	336.96	0.061	3.5	1.45×10^2	3130	107	12
DOBAMBC	367.732	390.2	0.058	3.2	1.25×10^2	3000	98	6
7O.6	343.301	353.5	0.029	1.6	2.58×10^2	4090	94	10
AMC-11	352.360	362.9	0.029	1.7	82	1380	33	10
MBRA8	322.918	329.2	0.019	0.9	71	790	14	13

^a ΔC_J in J/mole K.

^b \tilde{a} and \tilde{b} in J/mole.

HOBACPC: *n*-hexyloxybenzylidene-*p*'-amino-[2-chloro(*n*-propyl)]cinnamate.

2M45OBC: (2-methyl-butyl)-4'-(*n*-pentyloxybiphenyl)-4-carboxylate; *R*, racemic version; *C*, chiral version.

DOBAMBC: *p*-(*n*-decyloxybenzylidene)-*p*-amino-(2-methyl-butyl)cinnamate.

7O.6: N-(4-*n*-heptyloxybenzylidene)-4'-hexylaniline.

AMC-11: azoxy-4,4'-bi(*n*-undecyl- α -methylcinnamate).

MBRA8: *S*-4-O-(2-methyl-butyl) β -resorcyldiene-4'-*n*-octylaniline.

(See Appendix A for the molecular structure.)

was chosen as the normalization factor for the order parameter. From Eq. (3) one has tricritical dominated region for $|t|/t_0 \gg 1$, the asymptotic value of Ψ becomes $[b_0/(\sqrt{3t_0c_0})]^{1/2}|t|^{1/4}$. Now let us define $\tilde{\Psi}$, such that $\tilde{\Psi} = |t|^{1/4}$ for $|t|/t_0 \gg 1$. With this normalized order parameter $\tilde{\Psi}$, the free energy (Eq. 2) can be rewritten as

$$G = G_0 + \tilde{a}t\tilde{\Psi}^2 + \tilde{b}\tilde{\Psi}^4 + \tilde{c}\tilde{\Psi}^6. \quad (5)$$

Here, $\tilde{a} = a_1^{3/2}/\sqrt{3c_0}$, $\tilde{b} = a_1b_0/(3c_0)$, and $\tilde{c} = \tilde{a}/3$. One attractive feature of this new expression is that only \tilde{a} and \tilde{b} are independent coefficients because an additional condition, i.e., $b_0/(\sqrt{3t_0c_0}) = 1$ is imposed.¹⁷ The coefficient

\tilde{c} is proportional to \tilde{a} . Furthermore, \tilde{a} and \tilde{b} can be expressed in terms of the experimentally measurable quantities as follows: $\tilde{a} = 2T_{AC}(\Delta C_J)(t_0/3)^{1/2}$ and $\tilde{b} = \tilde{a}(t_0/3)^{1/2}$. Consequently, only heat-capacity data are required to determine the coefficient \tilde{a} and \tilde{b} . The systematic behavior of these coefficients (i.e., \tilde{a} and \tilde{b}) will be discussed in the next section.

IV. DATA REDUCTION AND DISCUSSIONS

The parameters obtained from heat-capacity measurements near the Sm *A*-Sm *C* (or Sm *C*^{*}) transitions of various compounds with the *I*-Sm *A*-Sm *C* (or Sm *C*^{*}) transi-

TABLE V. The parameters obtained from heat-capacity measurements near the Sm *A*-Sm *C* transitions of the pure compounds with the *I*-*N*-Sm *A*-Sm *C* transition sequence.

Compound	T_{AC} (K)	T_{NA} (K)	$1 - \frac{T_{AC}}{T_{NA}}$	$t_0 \times 10^3$	ΔC_J^a	\tilde{a}^b	\tilde{b}^b	References
2M4P9OBC	406.91	441	0.077	5.5	134	4670	200	6
7O.7	344.64	356.6	0.034	2.8	123	2600	80	14
7O.4	337.56	347.2	0.027	0.8	400	4400	70	10
8S5	328.18	336.1	0.024	7.3	47	1500	74	7,5
4O.7	323.11	329.8	0.022	1.3	65	870	18	10

^a ΔC_J in J/mole K.

^b \tilde{a} and \tilde{b} in J/mole.

2M4P9OBE: racemic 4-(2-methyl-butyl)phenyl-4-*n*-nonyloxybiphenyl-4-carboxylate.

7O.7: N-(4-*n*-heptyloxybenzylidene)-4'-*n*-heptylaniline.

7O.4: N-(4-*n*-heptyloxybenzylidene)-4'-*n*-butylaniline.

8S5: [O-4-(*n*-octyloxy)-*S*-4'-(*n*-pentyloxy)phenyl]thiolbenzoate.

4O.7: N-(4-*n*-butyloxybenzylidene)-4'-*n*-heptylaniline.

(See Appendix B for the molecular structure.)

TABLE VI. The parameters related to the Sm *A*-Sm *C* transition line of ($\overline{8S5}$ - $\overline{7S5}$) mixtures.

Mole % of $\overline{7S5}$ in $\overline{8S5}$	T_{NA} (K)		T_{AC} (K) ^b	$t_0 \times 10^{3b}$	$1 - \frac{T_{AC}}{T_{NA}}$	ΔC_J^c	\tilde{a}^d	\tilde{b}^d
0	336.085	A ^a	328.171	6.4	0.0235	46.6	1410	66
		B ^a	328.183	7.3				
15	331.990	B	326.618	4.5	0.0162	49.6	1250	48
31	326.172	A	322.603	1.8	0.0109	54.9	860	21
		B	322.612	4.7				
41	324.163	A	323.259	0.62	0.0018	89.3	1080	14
		B	323.271	1.6				
42	323.030	A	322.727	0.32	0.0009	303	2030	21
		B	322.737	0.58				

^aType of measurements: A, tilt angle; B, two-theta shift.

^bThe results obtained from fitting the tilt angle to Eq. (3) (Ref. 18).

^cUnits in J/mole K (from Ref. 19).

^dUnits in J/mole.

tion sequence or with the *I-N-SmA-SmC* transition sequence and along the Sm *A*-Sm *C* transition line of ($\overline{8S5}$ - $\overline{7S5}$) mixtures are shown in Tables IV, V, and VI, respectively. To our knowledge, these are the lists of all liquid-crystal compounds on which careful heat-capacity measurements have been carried out near their Sm *A*-Sm *C* (or Sm *C*^{*}) transition. The solid dots in Fig. 1 are the plots of the coefficient \tilde{a} and \tilde{b} versus $(1 - T_{AC}/T_{IA})$ for all the compounds listed in Table IV except the compound 7O.6. The abnormal behavior in the coefficient \tilde{a} and \tilde{b} of 7O.6

may be because of the relatively large heat-capacity jump (ΔC_J) at the transition temperature.¹⁰ The dimensionless parameter t_0 of 7O.6 follows the general trend⁴ for the rest of the compounds listed in Table IV. Figure 1 clearly indicates that both \tilde{a} and \tilde{b} decrease almost linearly as $(1 - T_{AC}/T_{IA})$ and MBRA8 seems to be close to a mean-field tricritical point ($\tilde{b} = 0$).

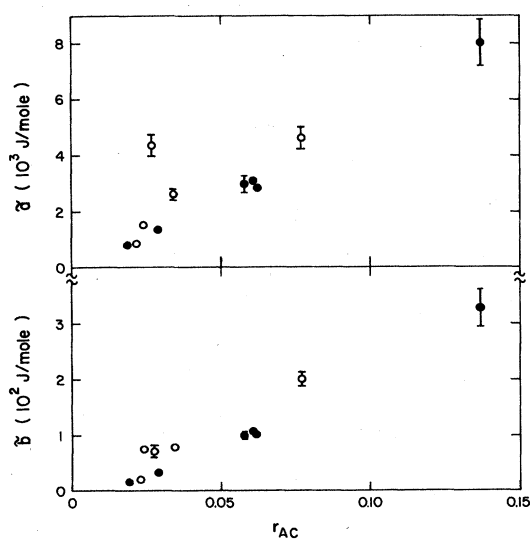


FIG. 1. Plots of the mean-field coefficient \tilde{a} and \tilde{b} vs r_{AC} for eleven pure liquid-crystal compounds, with Sm *A*-Sm *C* (or Sm *C*^{*}) transition. The solid dots are the compounds with *I*-Sm *A*-Sm *C* (or Sm *C*^{*}) transition sequence and $r_{AC} = (1 - T_{AC}/T_{IA})$. The open circles are the compounds with *I-N-SmA-SmC* transition sequence and $r_{AC} = (1 - T_{AC}/T_{NA})$.

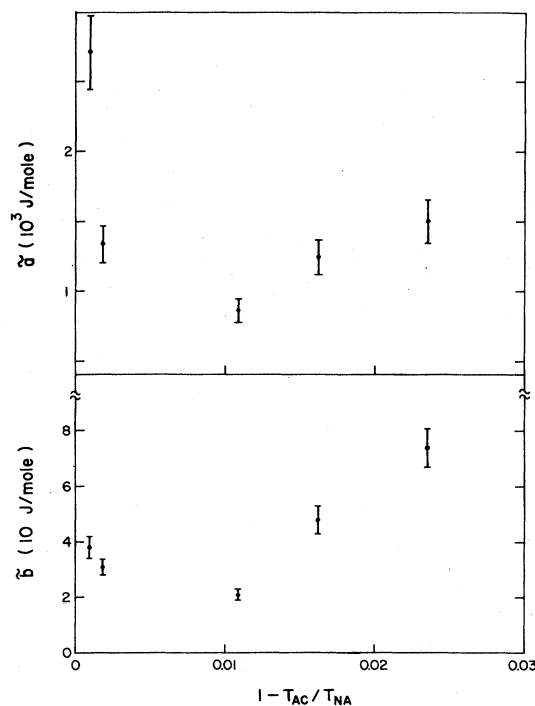


FIG. 2. Plots of the coefficient \tilde{a} and \tilde{b} vs $(1 - T_{AC}/T_{NA})$ for the mixture ($\overline{8S5}$ - $\overline{7S5}$) system along the Sm *A*-Sm *C* transition line.

field tricritical point ($\tilde{b}=0$).

From Table V, one can immediately realize that t_0 behaves relatively irregularly with the size of the SmA-phase range. However, the new set of mean-field coefficients, i.e., \tilde{a} and \tilde{b} seems to decrease as $(1-T_{AC}/T_{NA})$. Again, they vary systematically with the size of the SmA temperature range. The open circles in Fig. 1 show the variation of \tilde{a} and \tilde{b} with $(1-T_{AC}/T_{NA})$ for all the compounds listed in Table V. The data roughly follow the same trend as the compounds with the *I*-SmA-SmC (or SmC*) transition sequence but with much larger scattering. Furthermore, the existence of the nematic phase seems to increase the value of \tilde{a} and \tilde{b} , but no systematic effect due to the size of the nematic range can be identified.

In Fig. 2, the coefficient \tilde{a} and \tilde{b} are plotted as functions of $(1-T_{AC}/T_{NA})$, with t_0 being determined from the fitting two-theta shift data to Eq. (3).²⁰ As the SmA temperature range decreases, although the parameter t_0 shows a monotonical decrease,³ the normalized coefficient \tilde{a} and \tilde{b} seem to decrease and then increase. This is caused by the large increase in the heat-capacity jump¹⁹ near the NAC point at which the nematic, smectic-A, and smectic-C phase coexist. Consequently, the increase in \tilde{a} and \tilde{b} may be attributed to the fluctuations near the NAC multicritical point.²¹ Thus far all the existing theories²² for the NAC point fail to provide any indication of this increase. Careful data analysis on the existing heat-capacity data¹⁹ should shed further light on this important NAC multicritical point.

IV. CONCLUSION

Extensive data have been presented. The results clearly indicate that the SmA temperature range play an essential role in determining the mean-field coefficients of SmA-SmC (or SmC*) transition. This general behavior is further strengthened by the fact that among all twelve single-component liquid-crystal compounds reported here, there are seven different aromatic arrangements in the central parts of the molecules. See the Appendixes A and B for the molecular structural formula. Furthermore, our analyses seem to suggest that the smallness of t_0 or relative importance of the c_0 term in the mean-field free-energy expansion is directly related to the size of the SmA temperature range.

Series of phase transitions usually occur in a relative narrow temperature range in many liquid-crystal compounds. Thus phase transitions between mesophases provide a unique opportunity to study the effect of one transition on the other. Unlike relatively intriguing *N*-SmA transition, SmA-SmC (or SmC*) transition is relatively simple and can be well described by the extended mean-field free-energy expression proposed by Huang and

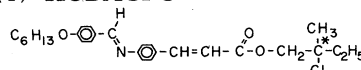
Viner.⁶ A microscopic theory which can explain the distinct feature associated with the SmA-SmC (or SmC*) transition, i.e., the mean-field-like transition with a large c_0 term, may be one of the good starting points to understand the other phase transitions between mesophases in liquid-crystal compounds.

ACKNOWLEDGMENTS

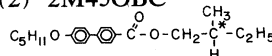
It is a pleasure to thank C. Campbell, R. A. Klemm, C. R. Safinya, G. Grinstein, and J. Toner for helpful discussions and suggestions. This work was partially supported by the National Science Foundation, Solid State Chemistry Program, Grant No. DMR-84-04945, and a grant from the Center for Microelectronic and Information Sciences (MEIS), University of Minnesota.

APPENDIX A: MOLECULAR STRUCTURE OF COMPOUNDS WITH *I*-SmA-SmC (or SmC*) TRANSITION

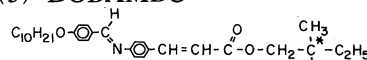
(1) HOBACPC



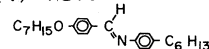
(2) 2M45OBC



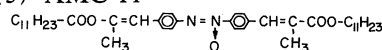
(3) DOBAMBC



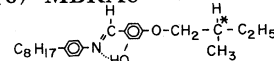
(4) 7O.6



(5) AMC-11

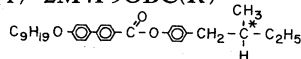


(6) MBRA8

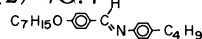


APPENDIX B: MOLECULAR STRUCTURE OF COMPOUNDS WITH *I*-N-SmA-SmC TRANSITION

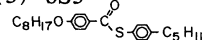
(1) 2M4P9OBC(R)



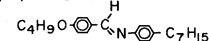
(2) 7O.4



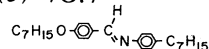
(3) 8S5



(4) 4O.7



(5) 7O.7



*Present address: Energy Conversion Devices, Troy, Michigan.

¹J. Thoen, H. Marynissen, and W. Van Dael, Phys. Rev. Lett. 52, 204 (1984).

²B. M. Ocko, R. J. Birgeneau, J. D. Litster, and M. E. Neubert, Phys. Rev. Lett. 52, 208 (1984).

³C. C. Huang and S. C. Lien, Phys. Rev. Lett. 47, 1917 (1981).

⁴S. C. Lien and C. C. Huang, Phys. Rev. A 30, 624 (1984).

⁵C. C. Huang and S. C. Lien, in *Multicritical Phenomena*, in Vol. 106 of the *Proceedings of the North Atlantic Treaty Organization Advanced Studies Institute*, edited by R. Pynn and

- A. Skjeltorp (Plenum, New York, 1984), Ser. B, p. 73.
- ⁶C. C. Huang and J. M. Viner, *Phys. Rev. A* **25**, 3385 (1982).
- ⁷C. A. Shantz and D. L. Johnson, *Phys. Rev. A* **17**, 1504 (1978).
- ⁸C. R. Safinya, M. Kaplan, J. Als-Nielsen, R. J. Birgeneau, D. Davidov, J. D. Litster, D. L. Johnson, and M. Neubert, *Phys. Rev. B* **21**, 4149 (1980).
- ⁹R. J. Birgeneau, C. W. Garland, A. R. Kortan, J. D. Litster, M. Meichle, B. M. Ocko, C. Rosenblatt, L. J. Yu, and J. Goodby, *Phys. Rev. A* **27**, 1251 (1983).
- ¹⁰M. Meichle and C. W. Garland, *Phys. Rev. A* **27**, 2624 (1983).
- ¹¹S. C. Lien, J. M. Viner, C. C. Huang, and N. W. Clark, *Mol. Cryst. Liq. Cryst.* **100**, 145 (1983).
- ¹²S. C. Lien, C. C. Huang, and J. W. Goodby, *Phys. Rev. A* **29**, 1371 (1984).
- ¹³S. C. Lien, C. C. Huang, T. Carlsson, I. Dahl, and S. T. Lagerwall, *Mol. Cryst. Liq. Cryst.* **108**, 148 (1984).
- ¹⁴J. Theon and G. Seynhaeve, *Abstracts of the Tenth International Liquid Crystal Conference* (York, United Kingdom, 1984) (unpublished).
- ¹⁵C. Rosenblatt and J. D. Litster, *Phys. Rev. A* **26**, 1809 (1982).
- ¹⁶In this section we are going to discuss the best choice of the unit for Ψ , thus a_1 cannot be set equal to one. Consequently, the numerical values of b_0 and c_0 must be different from those in Sec. II.
- ¹⁷If the SmC (or SmC*) existed at the absolute zero temperature and still could be described by Eq. (2), then the condition $b_0/(\sqrt{3}t_0c_0)$ would imply a normalization of order parameter at finite temperature with respect to the saturated order parameter.
- ¹⁸C. R. Safinya, R. J. Birgeneau, J. D. Litster, and M. E. Neubert, *Phys. Rev. Lett.* **47**, 668 (1981); C. R. Safinya, Ph.D. thesis, MIT, 1981.
- ¹⁹R. DeHoff, R. Biggers, D. Brisbin, and D. L. Johnson, *Phys. Rev. A* **25**, 472 (1982).
- ²⁰The two-theta shift measures the smectic layer spacing in the SmC phase just like the power pattern in x-ray crystallography. Because of the formation of SmC multidomain is unavoidable by using the magnetic field to align the liquid-crystal molecules, this measurement is less susceptible to defects than the tilt-angle measurements. Consequently, we plot the data determined by two-theta shift measurements only.
- ²¹C. R. Safinya, L. J. Martinez-Miranda, M. Kaplan, J. D. Litster, and R. J. Birgeneau, *Phys. Rev. Lett.* **50**, 56 (1983); S. Witanachchi, J. Huang, and J. T. Ho, *ibid.* **50**, 594 (1983).
- ²²H. Chen and T. Lubensky, *Phys. Rev. A* **14**, 1202 (1976); K. Chu and W. McMillan, *ibid.* **15**, 1181 (1977); L. Benguigui, *J. Phys. (Paris). Colloq.* **40**, C3-222 (1979); C. C. Huang and S. C. Lien, Ref. 3; G. Grinstein and J. Toner, *Phys. Rev. Lett.* **51**, 2386 (1983).